Effects of charge and dipole on flatband voltage in an MOS device with a Gd-doped HfO_2 dielectric*

Han Kai(韩 锴)[a)b)†], Wang Xiao-Lei(王晓磊)[b)], Yang Hong(杨 红)[b)], and Wang Wen-Wu(王文武)[b)]

[a)] *Department of Physics and Electronic Science, Weifang University, Weifang* 261061, *China*
[b)] *Key Laboratory of Microelectronics Devices & Integrated Technology, Institute of Microelectronics, Chinese Academy of Sciences, Beijing* 100029, *China*

(Received 29 March 2013; revised manuscript received 31 May 2013)

Gd-doped HfO_2 has drawn worldwide interest for its interesting features. It is considered to be a suitable material for N-type metal-oxide-semiconductor (MOS) devices due to a negative flatband voltage (V_{fb}) shift caused by the Gd doping. In this work, an anomalous positive shift was observed when Gd was doped into HfO_2. The cause for such a phenomenon was systematically investigated by distinguishing the effects of different factors, such as Fermi level pinning (FLP), a dipole at the dielectric/SiO_2 interface, fixed interfacial charge, and bulk charge, on V_{fb}. It was found that the FLP and interfacial dipole could make V_{fb} negatively shifted, which is in agreement with the conventional dipole theory. The increase in interfacial fixed charge resulting from Gd doping plays a major role in positive V_{fb} shift.

Keywords: high-k dielectric, $HfGdO_x$, interface dipole, flatband voltage shift

PACS: 77.55.D–, 73.40.Qv **DOI:** 10.1088/1674-1056/22/11/117701

1. Introduction

The continuous scaling down of metal-oxide-semiconductor (MOS) transistors makes it imperative to replace the conventional SiO_2/poly-Si structure with a high dielectric constant (high-k) dielectric/metal gate stack.[1–4] As a high-k dielectric, HfO_2 is widely used because of its overwhelming advantages.[5] However there still exist some challenges, such as the enhancement of the k value of HfO_2 and the threshold voltage (V_{th}) control. Generally, band edge metal gates are needed to obtain a low V_{th} for bulk CMOS application.[6] It was reported that introducing lanthanide elements or their compounds into HfO_2 can make flatband voltage V_{fb} negatively shift accompanied by an enhancement in the k value of HfO_2.[7–11] It is mostly believed that interface dipoles at the high-k/SiO_2 interface play a dominant role in V_{fb} modulation. Regarding the origin of the interface dipole, some models have been proposed, such as the electronegativity model and the oxygen areal density difference model.[12,13] Among all lanthanide elements, Gd has attracted extensive interests because Gd_2O_3 has many advantages, including thermodynamic stability on Si up to 1000 °C, comparable dielectric constant (∼20) to monoclinic HfO_2, and larger conduction and valence band offsets (∼ 2 eV).[14–16] In the present work, the effect of Gd doping into HfO_2 is systematically investigated.

2. Experiment

MOS capacitors with a W/TiN/$HfGdO_x$/terraced-SiO_2/n-Si structure were fabricated. Firstly, ∼ 20 nm-thick SiO_2 film was thermally grown on diluted HF-last n-type Si wafers (arsenic, 1.1×10^{15} cm^{-3}) by dry-oxidation technology. The thick SiO_2 film was wet etched to have a terraced structure. $HfGdO_x$ layers with fixed thicknesses (4 nm, 6 nm, 8 nm, 10nm, and 12 nm respectively) were deposited on the terraced SiO_2 by co-sputtering of targets HfO_2 and Gd_2O_3. The sputtering power for HfO_2 was 120 W, while the sputtering power for Gd_2O_3 was 90 W. Then a 30 nm-thick TiN film was deposited on the $HfGdO_x$ dielectric by sputtering, followed by depositing a 50 nm-thick sputtered W film. After back oxide removal by diluted HF, Al metallization and N_2 annealing at 400 °C for 50 min were performed. A sample with 12-nm pure HfO_2 was also fabricated with the same flow. In addition, a control sample with W/TiN/terraced-SiO_2/Si structure was also prepared to examine the fixed charge at the SiO_2/Si interface region. The C–V characteristics of the capacitors were measured at a frequency of 1 MHz and fitted by the QMCV model.[17]

3. Results and discussion

The typical C–V characteristics for the sample with W/TiN/12-nm-thick $HfGdO_x$/terraced-SiO_2/n-Si structure are shown in Fig. 1. The inset is the schematic diagram of the sample. Well behaved C–V characteristics are observed.

*Project supported by the National Science and Technology Major Project of the Ministry of Science and Technology of China (Grant No. 2009ZX02035) and the National Natural Science of China (Grant Nos. 61176091 and 50932001).

†Corresponding author. E-mail: hankai@ime.ac.cn

© 2013 Chinese Physical Society and IOP Publishing Ltd

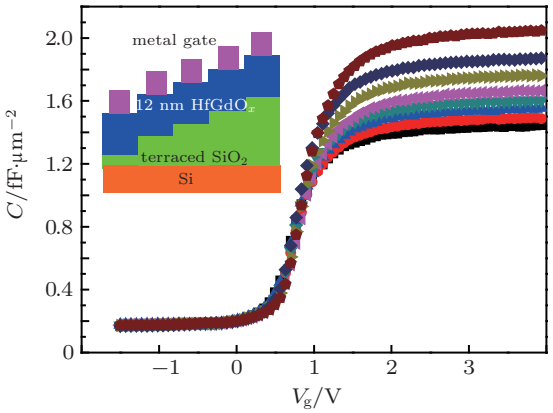


Fig. 1. (color online) Typical C–V plots for the sample with W/TiN/12-nm-thick HfGdO$_x$/terraced-SiO$_2$/n-Si structure. The inset is the schematic diagram of the sample.

Figure 2 shows the V_{fb} versus equivalent oxide thickness (EOT) curves for the samples with 12-nm HfGdO$_x$ and with 12-nm HfO$_2$. An obvious positive V_{fb} shift exists for the Gd-doped sample compared with that of the pure HfO$_2$ sample. This is not in agreement with the traditional dipole model.[12] The same anomalous phenomenon was also reported at Ref. [18]. So we can conclude that there may be something wrong with the model or there is something overlooked in the model. Among all contributing factors to V_{fb}, the impact of the fixed charge in bulk and at interface is neglected in the model. So, it is important to clarify the effect of each contributing factor, including Fermi level pinning (FLP), interface dipole, fixed bulk charge, and fixed interfacial charge.

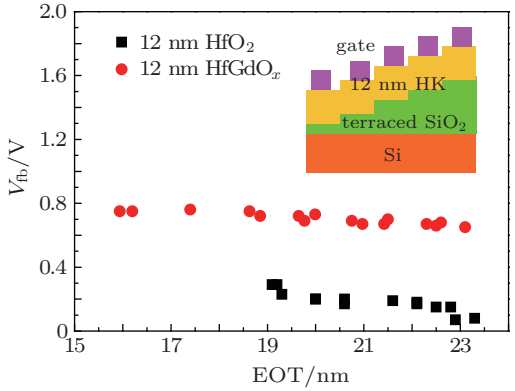


Fig. 2. (color online) The V_{fb} versus EOT for samples with and without Gd doping.

Figure 3 shows the V_{fb} versus EOT curve for the sample with W/TiN/terraced-SiO$_2$/n-Si structure. The inset is the schematic diagram of the sample. For the case without high-k dielectric, the relationship between V_{fb} and EOT can be expressed as

$$V_{fb} = \phi_{ms} - \frac{Q_{SiO_2,Si}T_E}{\varepsilon_0\varepsilon_{SiO_2}} - \frac{\rho_{bulk,SiO_2}T_E^2}{2\varepsilon_0\varepsilon_{SiO_2}}, \quad (1)$$

where ϕ_{ms} is the vacuum work function difference between the metal gate and the Si substrate, $Q_{SiO_2,Si}$ is the areal charge density (per unit area) at the SiO$_2$/Si interface, ρ_{bulk,SiO_2} is the bulk charge density (per unit volume) in SiO$_2$, ε_0 and ε_{SiO_2} are the vacuum permittivity and the relative permittivity of SiO$_2$, respectively, and T_E is the EOT. As shown in Fig. 3, the good linear fitting of V_{fb}–EOT indicates that ρ_{bulk,SiO_2} is small enough and its effect on V_{fb} can be negligible. By fitting the V_{fb}–EOT data, $Q_{SiO_2,Si} = 4.68\times10^{11}$ cm^{-2} and $\phi_{ms} = 0.655$ V are obtained.

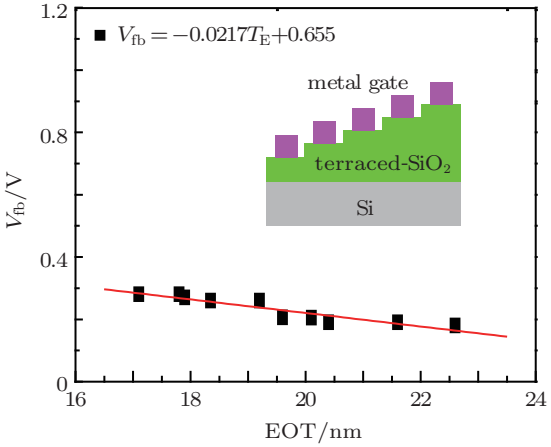


Fig. 3. (color online) The V_{fb} versus EOT for the sample with a W/TiN/terraced-SiO$_2$/n-Si structure. The inset is the schematic diagram of the sample.

Figure 4 shows the V_{fb} versus EOT curves for the samples with a W/TiN/fixed HfGdO$_x$/terraced-SiO$_2$/n-Si structure. Here, the thickness of the HfGdO$_x$ film is varied from 4 nm to 12 nm. For the case with a HfGdO$_x$ dielectric, the relationship between V_{fb} and EOT can be expressed by

$$\begin{aligned} V_{fb} = {} & \phi_{ms} - \frac{Q_{SiO_2,Si}T_E}{\varepsilon_0\varepsilon_{SiO_2}} - \frac{\rho_{bulk,SiO_2}T_E^2}{2\varepsilon_0\varepsilon_{SiO_2}} - \frac{Q_{HK,SiO_2}T_{HK}}{\varepsilon_0\varepsilon_{HK}} \\ & - \frac{\rho_{bulk,HK}T_{HK}^2}{2\varepsilon_0\varepsilon_{HK}} + \frac{\rho_{bulk,SiO_2}\varepsilon_{SiO_2}T_{HK}^2}{2\varepsilon_0\varepsilon_{HK}^2} \\ & + \Delta V_{HK,SiO_2} + \Delta V_{metal,HK}, \end{aligned} \quad (2)$$

where Q_{HK,SiO_2} is the areal charge density (per unit area) at the HfGdO$_x$/SiO$_2$ interface, T_{HK} and ε_{HK} are the physical thickness and the relative permittivity of the HfGdO$_x$ film, respectively, $\rho_{bulk,HK}$ is the bulk charge density (per unit volume) in the HfGdO$_x$ film, which is supposed to be a constant over the whole film region, $\Delta V_{HK,SiO_2}$ and $\Delta V_{metal,HK}$ represent the possible moments of V_{fb} shift caused by the electric dipole at the HfGdO$_x$/SiO$_2$ interface and the FLP at the metal gate/HfGdO$_x$ interface, respectively. As shown in Fig. 4, ρ_{bulk,SiO_2} can also be negligible because of the good linear fitting of V_{fb}–EOT curves in this case, which coincides with ρ_{bulk,SiO_2} described in Fig. 3. So, Eq. (2) can be rewritten as

$$\begin{aligned} V_{fb} = {} & \phi_{ms} - \frac{Q_{HK,SiO_2}T_{HK}}{\varepsilon_0\varepsilon_{HK}} - \frac{\rho_{bulk,HK}T_{HK}^2}{2\varepsilon_0\varepsilon_{HK}} \\ & + \Delta V_{HK,SiO_2} + \Delta V_{metal,HK} - \frac{Q_{SiO_2,Si}T_E}{\varepsilon_0\varepsilon_{SiO_2}}. \end{aligned} \quad (3)$$

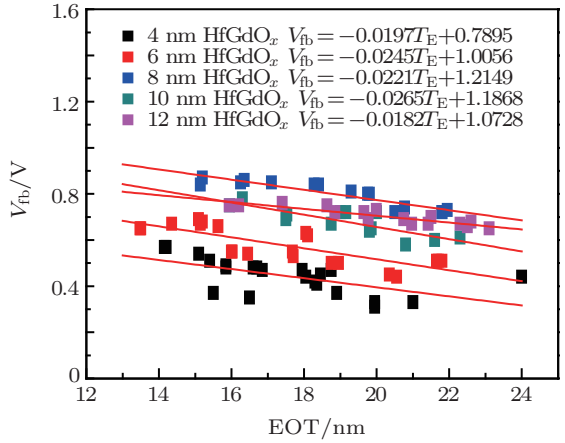


Fig. 4. (color online) The V_{fb}–EOT curves for the samples with different thicknesses of HfGdO$_x$.

From Eq. (3) and Fig. 4, it can be seen that the intercepts (I) of the V_{fb} versus EOT curves are obviously related with T_{HK}, and the dependence of I on T_{HK} can be expressed as

$$I = -\frac{Q_{HK,SiO_2}T_{HK}}{\varepsilon_0\varepsilon_{HK}} - \frac{\rho_{bulk,HK}T_{HK}^2}{2\varepsilon_0\varepsilon_{HK}} + \Delta V_{HK,SiO_2} + \Delta V_{metal,HK} + \phi_{ms}. \quad (4)$$

Herein the unknown constant ε_{HK} can be extracted from the EOT–T_{HK} relationship shown in Fig. 5. The inset in Fig. 5 shows the schematic diagram of the sample with metal gate / terraced-HfGdO$_x$ / fixed-SiO$_2$ / Si structure. Here, the terraced-HfGdO$_x$ represents the HfGdO$_x$ films with different thicknesses deposited on the wafers with the same $\sim$ 20 nm-thick SiO$_2$/Si structure. The relative dielectric constant for Gd-doped HfO$_2$ extracted here is 20.8, while the relative dielectric constant for pure HfO$_2$ is 18,[19] which proves the dielectric enhancement of Gd doping.[14]

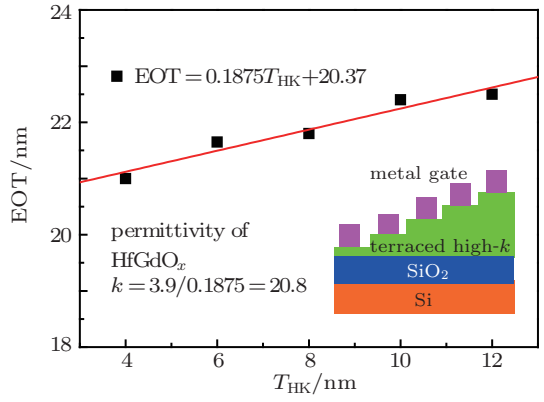


Fig. 5. (color online) The EOT–T_{HK} plot for the extraction of the permittivity of HfGdO$_x$. The inset is the schematic diagram of the sample.

The relationship of I and T_{HK} extracted from Fig. 4 is shown in Fig. 6. By comparing the fitting equation of the I–T_{HK} data with Eq. (4), we can obtain

$$Q_{HK,SiO_2} = -2.73\times10^{13}\ \text{cm}^{-2},$$
$$\rho_{bulk,HK} = 2.97\times10^{19}\ \text{cm}^{-3},$$
$$\Delta V_{HK,SiO_2} + \Delta V_{metal,HK} = -0.798\ \text{V}.$$

For pure HfO$_2$,[19]

$$Q_{HK,SiO_2} = -1.15\times10^{13}\ \text{cm}^{-2},$$
$$\rho_{bulk,HK} = 9.76\times10^{18}\ \text{cm}^{-3},$$
$$\Delta V_{HK,SiO_2} + \Delta V_{metal,HK} = -0.38\ \text{V}.$$

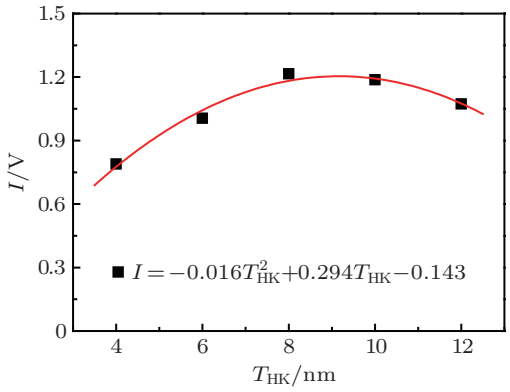


Fig. 6. (color online) Relationship of I and T_{HK}.

As for the effects of FLP and interfacial dipole, we can find that Gd doping actually results in about 400 mV negative V_{fb} shift. It proves that Gd doping can indeed issue in negative dipole and FLP, which is in good agreement with the traditional model. A relatively larger bulk charge density can also make V_{fb} negatively shifted. However the negative charge at the HfGdO$_x$ and SiO$_2$ interface counteracts the effects of FLP and interfacial dipole, which makes the V_{fb} positively shifted. The larger charge densities both in bulk and at interface are considered to be due to cosputtering of HfO$_2$ and Gd$_2$O$_3$ without any subsequent treatment which may result in more defects, more dangling bonds, and severe mismatches.

4. Conclusion

An anomalous positive V_{fb} shift was observed when Gd was doped into HfO$_2$. The cause for this phenomenon was systematically investigated. The effects of FLP, interfacial dipole, fixed bulk charge, and interfacial charge on V_{fb} were separated. It was found that a larger interfacial charge density at the HfGdO$_x$ and SiO$_2$ interface is responsible for the anomalous positive V_{fb} shift. The effects of FLP and interfacial dipole are to make V_{fb} negatively shifted, which is in agreement with the conventional dipole model. So it is important to recognize the role of various charge and take steps to avoid such effects, such as appropriate post deposition annealing.

References

[1] Wilk G D, Wallace R M and Anthony J M 2001 *J. Appl. Phys.* **89** 5243
[2] Zhao Y, Toyama M, Kita K, Kyuno K and Toriumi A 2006 *Appl. Phys. Lett.* **88** 072904

[3] Chau R, Brask J, Datta S, Dewey G, Doczy M, Doyle B, Kavalieros J, Jin B, Metz M, Majumdar A and Radosavljevic M 2005 *Microelectronic. Eng.* **80** 1

[4] Huang L, Huang A P, Zheng X H, Xiao Z S and Wang M 2012 *Acta Phys. Sin.* **61** 137701 (in Chinese)

[5] Tan T T, Liu Z T and Li Y Y 2011 *Chin. Phys. Lett.* **28** 086803

[6] Narayanan V, Paruchuri V K and Bojarczuk N A 2006 *Dig. Tech. Pap. Symp. VLSI Tech*. June 13–17, 2006 Hawaii USA, p. 224

[7] Alshareef H N, Quevedo-Lopez M A, Wen H C, Harris R, Kirsch P, Majhi P, Lee B H and Jammy R 2006 *Appl. Phys. Lett.* **89** 232103

[8] Yu H Y, Chang S Z and Veloso A 2007 *Dig. Tech. Pap. Symp. VLSI Technol.* June 12–16, 2007 Kyoto Japan, p. 18

[9] Kirsch P D, Sivasubramani P and Huang J 2008 *Appl. Phys. Lett.* **92** 092901

[10] Wang W W, Mizubayashi W, Akiyama K, Nabatame T and Toriumi A 2008 *Appl. Phys. Lett.* **92** 162901

[11] Takahashi H, Minakata H, Morisaki Y, Xiao S Q, Nakabayashi M, Nishigaya K, Sakoda T, Ikeda K, Morioka H, Tamura N, Kase M and Nara Y 2009 *Tech. Dig. Int. Electron Devices Meet.* December 7–9, 2009 Baltimore USA, p. 427

[12] Sivasubramani P, Böscke T S and Huang J 2007 *Dig. Tech. Pap. Symp. VLSI technol.* June 12–16, 2007 Kyoto Japan, p. 68

[13] Kita K and Toriumi A 2009 *Appl. Phys. Lett.* **94** 132902

[14] Xiong Y H, Tu H L, Du J, Ji M, Zhang X Q and Wang L 2010 *Appl. Phys. Lett.* **97** 012901

[15] Losovyj Y B, Ketsman I, Sokolov A, Belashchenko K D, Dowben P A, Tang J K and Wang Z J 2007 *Appl. Phys. Lett.* **91** 132908

[16] Ketsman I, losovyj Y B, Sokolov A, Tang J, Wang Z, Belashchenko K D and Dowben P A 2007 *Appl. Phys. A* **89** 489

[17] Berkeley Device Group

[18] Ji M, Wang L, Xiong Y H and Du J 2010 *J. Rare Earth* **28** 396

[19] Wang X L, Han K, Wang W W, Ma X L, Chen D P, Zhang J, Du J, Xiong Y H and Huang A P 2010 *Appl. Phys. Lett.* **97** 062901